LA-UR-12-24414
Approved for public release; distribution is unlimited.

Title:	LANL Activities in Model Benchmarking and Thermal Test Design Calculations
Author(s):	Stauffer, Philip H. Harp, Dylan R. Robinson, Bruce A.
Intended for:	DOE NE deliverable Report

LANL Milestone M4FT-12LA0806091

LANL Activities in Model Benchmarking and Thermal Test Design Calculations

August 31, 2012

Philip Stauffer
Dylan Harp
Bruce Robinson

I. Executive Summary

This report summarizes the work of Los Alamos National Laboratory (LANL) on simulations related to nuclear waste storage in a salt repository. The work is primarily designed to show that the LANL developed porous flow simulator, FEHM, can reproduce results of experiments performed at the Waste Isolation Pilot Plant (WIPP) under the restricted conditions in which the system can be modeled assuming thermal and hydrologic processes dominate the behavior. As such, the work is a preliminary effort at simulating the fluid flow and heat transport processes, before treating the fully coupled thermal-mechanical-hydrologic-chemical (TMHC) coupled processes in the future.

The experiments chosen for the benchmarking exercise were originally performed to gather data and insight into how high level nuclear waste will impact salt in a repository setting. These experiments involved drilling boreholes into the floors of WIPP rooms and emplacing heaters in the holes. During the experiments, water flow from the surrounding salt into the boreholes was measured.

The benchmarking presented in this report explores the ability of the numerical simulations to accurately capture several aspects of the experiments. The report begins with a section wherein FEHM is used to recreate analytical model results associated with the experimental effort. This step is crucial to give confidence that FEHM is working for type of simulations needed to correctly model the migration of brine in a salt repository. Next, FEHM is used to simulate the experimental boreholes during the period before heating occurs. Then, simulations are performed to explore the impacts of increased temperature on the system.

The final section of the report describes initial creation of a three dimensional drift scale heater simulation in a hypothetical salt repository. These proof of concept simulations show the direction that LANL will take in moving from the benchmark heater scale simulations to larger repository scale simulations. Although these final simulations are performed with no water flow, the results are informative and provide the basis for discussion of likely processes that will be seen in the next phase of the effort when water and water vapor are included.

II. Background on the WIPP Experiments

The benchmarking presented in this report explores the ability of the numerical simulations to accurately recreate results originally obtained in the mid 1980s. The experiments we consider were performed starting in April 1985. The experimental results and subsequent analysis through analytical modeling are summarized in a 1988 Sandia report entitled “Brine Inflow to WIPP Disposal Rooms: Data, Modeling, and Assessment”.

The experiments were performed to gain understanding on how much water may be expected to flow into a void created by drilling in bedded salt at WIPP and the impacts of heat on increasing water release.

Boreholes in the range of 30-36 inch diameter were drilled into the floors of two WIPP rooms and used for the brine inflow experiments. Results from the WIPP experiments suggest that before heating, inflow rates of 5-15 g/day are typical, whereas after heating brine inflow rates increased to maximum before decreasing (Figure 1).

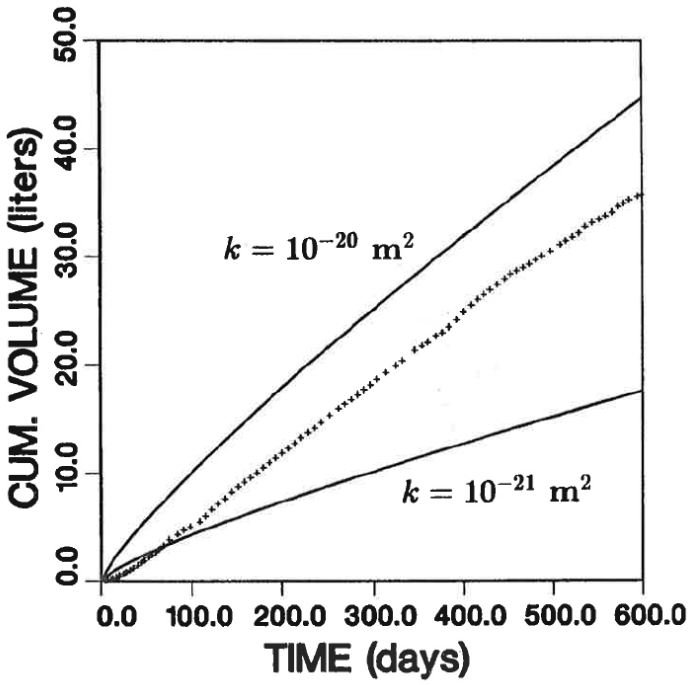

Figure II.1 Brine production data (plus signs) from Nowak et al., 1988.

III. Brief introduction to FEHM

The Finite Element Heat and Mass Transfer Code, FEHM, has been developed by LANL for more than 30 years (Zyvoloski, 2007). The code started as a tool to simulate the hot-dry rock experiments, but has grown over the years to include unsaturated flow, reactive chemistry, stress, and carbon dioxide (fehm.lanl.gov). FEHM has been used in more than 100 peer reviewed publications (FEHM 2012). FEHM uses a finite volume method for solving multiphase flow and transport, while using a finite element formulation for the fully coupled stress solutions. Capabilities pertinent to the salt simulations presented in this report include the ability to run fully coupled heat and mass transfer on both 2-D radial and 3-D numerical meshes. Simulations presented herein make use of a simplified pressure/porosity relationship that allows us to begin work on the impacts of changing

pore pressure on flow. However the fully coupled stress/flow solution will permit more sophisticated simulations as the project evolves. Additionally, the reactive chemistry components of the code will also be quite useful because project plans call for study of water source terms associated with pressure within fluid inclusions that can break salt crystals. The reactive chemistry section of the code will also allow us to explore clay hydration/dehydration reactions and their impacts on repository performance.

In addition to standard heat-mass-stress, FEHM has been modified to include two models for salt thermal conductivity as a function of temperature (Clayton and Gable, 2009). First, intact salt follows the Munson et al. (1990) relationship:

$$\lambda_{salt}(T) = \lambda_{300}\left(\frac{300}{T}\right)^{\gamma}$$

where λ_{300} is the thermal conductivity of salt at T = 300 K (5.4 W/m K), and γ is a material constant of 1.14. The thermal conductivity of crushed salt is based on the BAMBUS II study (Bechtold et al., 2004) and results in the following equation (From Clayton and Gable, 2009):

$$\lambda_{c-salt}(T) = k_{cs}(\varphi)\left(\frac{300}{T}\right)^{\gamma}$$

With the porosity (φ) dependent thermal conductivity k_{cs} as:

$$k_{cs}(\varphi) = (-270\varphi^4 + 370\varphi^3 - 136\varphi^2 + 1.5\varphi + 5) \cdot 1.08$$

IV. Benchmarking FEHM against analytical models from 1988 WIPP report

a. Isothermal Analytical

Deal and Case (1987) present graphical results for the total flux into 20 experimental boreholes excavated at the Waste Isolation Pilot Plant (WIPP). Nowak et al. (1988) assess the salt permeability at WIPP based on this data using an analytical model of transient Darcy flow in a porous medium. The basis of the model is the isothermal diffusion equation, defined as

$$\frac{\partial p}{\partial t} = c\nabla^2 p,$$

where p is the fluid pore pressure, c is the fluid diffusivity, and t is time. The fluid diffusivity c depends on permeability, fluid viscosity, and the elastic properties of the fluid and solid. The excavated borehole at depth is idealized in the model using an initial condition of constant pore pressure as

$$p(r, t = 0) = p_{0,}$$

where r is the radius from the center of the borehole and p_0 is the initial pressure. Boundary conditions set the pressure at zero at the borehole walls and p_0 at the far field as

$$p(a, t) = 0$$

and

$$\lim_{r\to\infty} p(r, t) = p_{0,}$$

where a is the borehole radius. Solving these equations for flux at the borehole wall (Crank, 1979) produces

$$q(a, t_*) = \frac{4kp_0}{\pi^2 \mu a} \int_0^\infty \frac{\exp(-u^2 t_*)}{\mathrm{J}_0^2(u) + \mathrm{Y}_0^2(u)} \frac{du}{u}$$

where k is permeability, μ is fluid viscosity, $t_*=ct/a^2$ is dimensionless time, and $\mathrm{J}_0(x)$ and $\mathrm{Y}_0(x)$ are zero-order Bessel functions of the first and second kind, respectively. Nowak et al. (1988) estimated permeabilities using this result and the data from Deal and Case (1987).

Assumptions in the analytical model include (1) the porous medium is saturated (Darcy flow), (2) a limitless interconnected network of pores exist extending out to the far field, (3) and the brine flow is radially symmetric.

i. FEHM representation of the isothermal analytical model

A numerical model was developed using FEHM. The borehole is idealized in the numerical model as a 2D radial slice of a 0.04 m radius borehole 0.01 m thick. The radial mesh spacing increases geometrically to a far field radius of 100 m. The numerical mesh uses an orthogonal grid with refinement close to the borehole, expanding geometrically to the far-field boundary at 100 m. Grid generation is automated to facilitate modifications to different borehole geometries (GRIDDER, 2012).Figure IV.1 shows the numerical mesh exaggerated in the vertical dimension with the pressure solution after 100 days of flow mapped onto the mesh in color. Pressure in the borehole at r=0.1 m is fixed at 0.1

MPa while the far-field boundary (100 m) is fixed at 10 MPa. In the simulations presented, the temperature of the isotheral solution was fixed to 3.0 C to capture the lower viscosity used in the analytical work presented in Nowak et al. (1988). This highlights the need to modify the viscosity dependence in FEHM to include the effects of high concentrations of salt. This will be one of the first tasks undertaken in the next stages of the project.

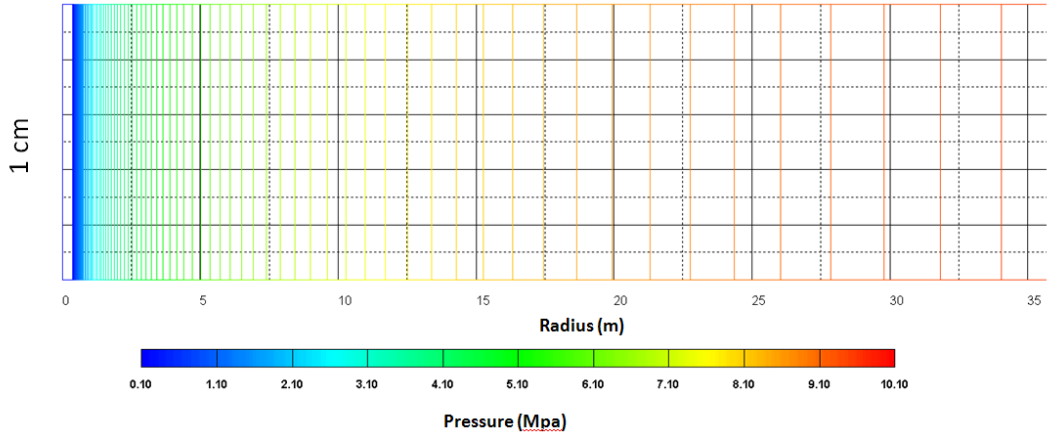

Figure VI.1 Numerical mesh for benchmarking simulations.

The FEHM simulation results are compared to the analytical solution above and presented in Figure IV.2. The simulator was run for several configurations of radius and results plotted in dimensionless space were able to correctly match the analytical solution (compare with Figure 1, Nowak et al. (1988)).

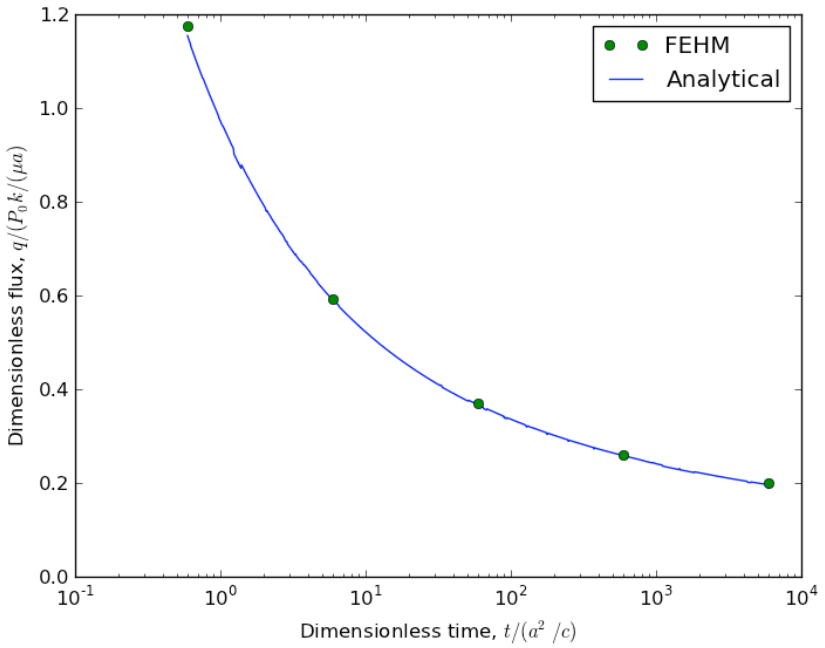

Figure IV.2 Comparison of analytical and numerical models of flux into an excavated borehole.

While the assumptions of the analytical model were imposed on the numerical model for benchmarking purposes, many of these assumptions are not required by the numerical model. The numerical model can be used to explore effects of unsaturated multiphase flow and a radially limited interconnected pore network (e.g. limited to a disturbed rock zone (DRZ) surrounding the borehole).

b. Heated Analytical

Nowak et al. (1988) present an analytical model of flow to a heated borehole considering the porous media as a linearly elastic skeleton. The basis of the model is the diffusion equation defined as

$$\frac{\partial p}{\partial t} - c\nabla^2 p = b' \frac{\partial \theta}{\partial t},$$

where p is the fluid pore pressure, c is the fluid diffusivity, b' is a source coefficient, ϑ is the temperature and t is time. The fluid diffusivity c depends on permeability, fluid viscosity, and the elastic properties of the fluid and solid.

For conduction-dominated problems, the solution of the pressure diffusion equation must be coupled with the heat equation

$$\frac{\partial \theta}{\partial t} - \kappa\nabla^2 \theta = 0,$$

where κ is the thermal diffusivity.

The initial and boundary conditions for temperature are

$$\theta(r, 0) = \theta_0,$$

$$\frac{\partial \theta}{\partial r}(a, t) = -\frac{q^h}{K},$$

and

$$\lim_{r\to\infty} \theta(r, t) = \theta_0,$$

where ϑ_0 is the initial temperature, a is the borehole radius, q^h is the heat flux at the borehole wall, and K is the thermal conductivity. Initial and boundary conditions for pressures are

$$p(r, 0) = p(a, t) = \lim_{r\to\infty} p(r, t) = 0.$$

The solution of these equations is

$$q(a, t_*) = -\frac{kb'q^h}{\mu KR(1 - R^2)} \frac{2}{\pi} \int_0^\infty \frac{\exp(-\omega^2 t_*)\,[\Phi J_1(\omega) - \Psi Y_1(\omega)]}{[J_1^2(R\omega) + Y_1^2(R\omega)][J_0^2(\omega) + Y_0^2(\omega)]} \frac{d\omega}{\omega},$$

where

$$\Phi = J_0(\omega)\Lambda_1 + Y_0(\omega)\Lambda_2,$$

$$\Psi = J_0(\omega)\Lambda_2 + Y_0(\omega)\Lambda_1,$$

$$\Lambda_1 = J_0(R\omega)Y_1(R\omega) - Y_0(R\omega)J_1(R\omega),$$

$$\Lambda_2 = J_0(R\omega)J_1(R\omega) + Y_0(R\omega)Y_1(R\omega),$$

and $R^2 = c/\kappa$ is the ratio of fluid and thermal diffusivities. Material property equations and typical values for WIPP are presented in Appendix A of Nowak et al. (1988). Following Nowak et al. (1988), we use a viscosity of 0.6×10^{-3} Pa s and fluid thermal expansion coefficient of 5.6×10^{-4} K^{-1}, corresponding to a temperature of 95°C, the measured temperature at the borehole wall of B042 at 100 days, the time of peak measured flux.

Figure IV.3.a presents a copy of Figure 3 from Nowak et al. (1988), displaying the measured cumulative brine inflow volume to borehole B042 and their simulated values using the equations above. Figure IV.3.b presents our simulated cumulative volumes calculated using the equations above and the same parameter values as listed in Nowak et al. (1988). Although the same equations and parameter values are used, it is apparent that our calculations do not agree with those from Nowak et al. (1988), where we simulate significantly less inflow. Further investigations into the formulations of these equations (e.g. McTigue (1985)) are required to uncover the source of this discrepancy.

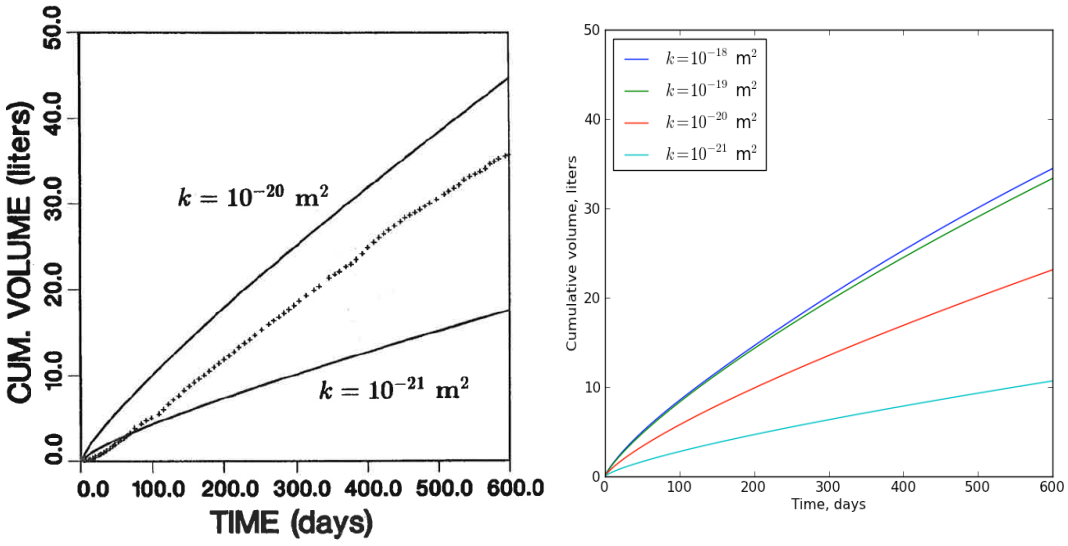

(a) (b)

Figure IV.3 Cumulative volume of brine inflow to borehole B042. Plot (a) is a copy of Figure 3 from Nowak et al. (1988) and plot (b) is a reproduction of the simulated values.

V. Benchmarking experimental results from the 1985 WIPP experiments

a. Isothermal phase FEHM vs Experimental data

According to Nowak et al. (1988), volumetric flux of 5-15 g/day were measured in borehole B042 prior to heating for at least two weeks. Figure V.1 presents analytical and

numerical simulations of volumetric flux into B042 for 100 days, where it is apparent that the flux remains in between 5 and 15 g/day from day 1 to around two weeks. The permeability in these simulations is $0.5x10^{-18}$ m^2. This indicates that permeability in B042 must be 2 orders of magnitude higher than for the smaller boreholes monitored in Deal and Case (1987) in order to simulate the volumetric flux observed in B042. Interestingly, the analytical model fits for isothermal flow fits very well with the calculated permeability that yields flows in the 5-15 g/day range. This result conflicts with the permeability estimates found in the heated analytical solution of Nowak (1988) and shows a logical inconsistency that needs to be addressed. Interestingly, the analytical results that fit the experimental data obtained by LANL for the heated case yield a similar permeability ($1x10^{-18}$ m^2) as we found for the isothermal part of the experiment. This suggests that the larger diameter boreholes may have higher near-field permeability than the small diameter boreholes. Such a difference could be the result of a larger damaged zone due to higher stresses and vibrations encountered when drilling large diameter boreholes.

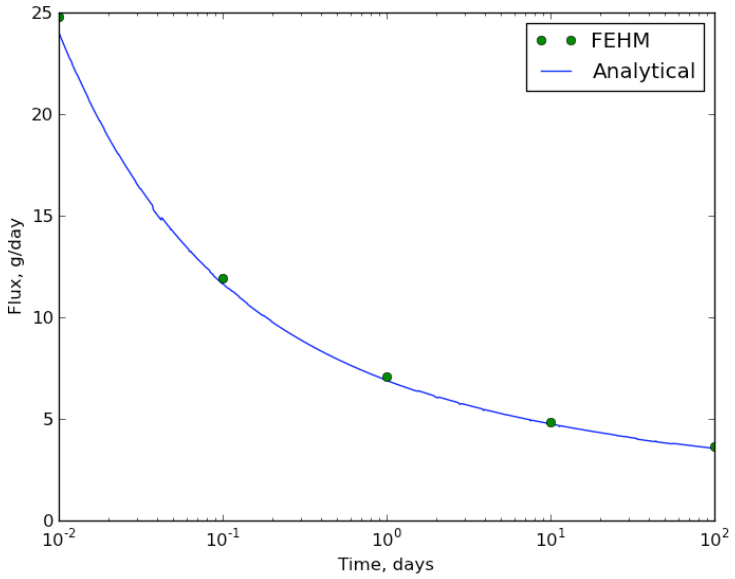

Figure V.1 Numerical and analytical simulation of non-heated volumetric flux into borehole B042 (Nowak et al. (1988)).

b. Heated phase FEHM vs Experimental data

Numerical simulations of brine inflow to a borehole in salt were performed using FEHM. Figure IV.4 presents the numerically simulated cumulative brine inflow into borehole B042 using FEHM. Achieving the plotted volumes required setting the permeability to $1.0x10^{-21}$ m^2 and reducing the solid expansivity by around 20 times its reported value ($1.2x10^{-4}$ K^{-1}; Nowak et al. (1988)).

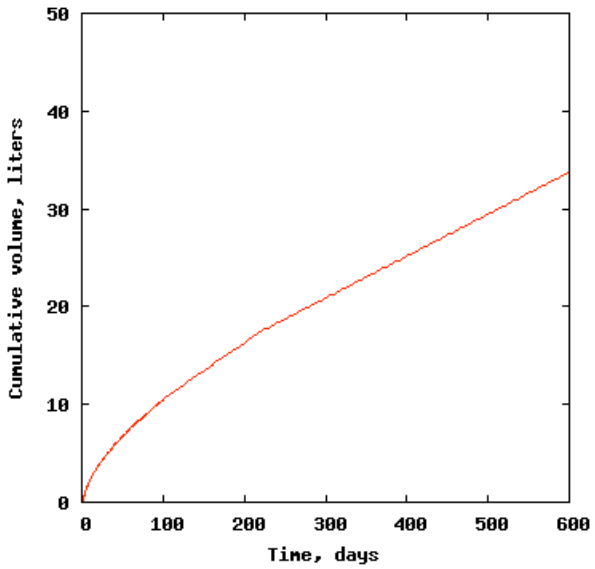

Figure IV.4 Numerically simulated cumulative brine inflow using FEHM.

The Gangi model for stress dependent properties is used (Gangi, 1978) where

$$\phi = \phi_0 \left[1 - \left(\frac{P_c}{P_x}\right)^m\right]$$

and

$$P_c = \sigma - P - \alpha E \Delta T,$$

where φ is the porosity, φ_0 is the initial porosity, P_c is the closure stress, P is the fluid pressure, σ is the *in situ* stress, α is the coefficient of thermal expansion of the rock, E is the Young's modulus, ΔT is the temperature change in the rock, and P_x and m are fitting parameters. Changes to permeability due to stress and temperature are modeled as

$$k = k_0 \left(\frac{\phi}{\phi_0}\right)^3,$$

where k is the current permeability and k_0 is the initial permeability.

By comparing Figure IV.4 with IV.3, it is apparent that the flux into the borehole is larger at earlier times than the observed or analytical flux. Attempts to reduce the initial numerically simulated flux, including allowing non-heated flux for 2 weeks and 3 months, as in the experiment (Nowak et al. 1988), proved unsuccessful in reducing the initial flux. The cause of the discrepancy between measured and numerically simulated inflow may be due to the use of the Gangi model. The feedback on permeability in the Gangi model does not allow modeling the cracking of salt as the temperature increases. Refinements to the stress dependent permeability are thus a critical need in the next phase of the LANL brine flow modeling.

VI. Drift scale heater tests

This section describes proof-of-concept calculations for a hypothetical drift scale heater experiment. The heater experiment is meant to show how thermally active nuclear waste might perturb the background temperature profiles within the repository. The calculations presented are done using heat flow only, with no water present. An immediate future goal of the current project is to take the benchmarked FEHM brine inflow results and build them into these drift scale heater simulations with a goal of better understanding of possible water migration during such thermal testing.

a. Drift scale heater test simulation design

A 3-D numerical mesh, shown in Figure VI.1, was created to include a section of a salt repository measuring 40 m x 40 m x 40 m. An experimental drift is located in the center of the domain, with five heaters spaced equally along the length of the drift. Run-of-mine (crushed) salt is backfilled on top of the heaters with angle of repose slopes forming on either end of the drift.

Table VI.1

	ft	m	Simulated
heater length	9	2.7432	2.5
drift width	11	3.3528	3.5
lateral salt width	38	11.5824	11.5
length	80	24.384	25
hight of crushed salt	10	3.048	3
depth below floor	10	3.048	3
above ceiling	10	3.048	3
lateral center to drift	43.5	13.2588	13
hight of salt + buffer	16	4.8768	5
Access tunnel height	13	3.9624	4
Access tunnel width	16	4.8768	5
half the length of the block	40	12.192	12
solid crused salt section N	20	6.096	6
edge of salt slope	34	10.3632	10.5

The experimental drift is centered at (0,0,0), and surrounded by access tunnels. Dimensions of the experimental drift, crushed salt backfill, access tunnels, and other aspects of the simulations are given in Table VI.1. This table shows actual dimensions in both feet and meters followed by the approximate equivalents that were used in the simulations. The numerical mesh maintains 0.5 m lateral spacing around the experimental drift with the same 0.5 m vertical to 3 m above and 3 m below the drift floor (Figure VI.2 and VI.3). Five heaters, shown in both Figures VI.2 and VI.3 have dimensions of 2.5m x 0.5m x 0.5m in XYZ space.

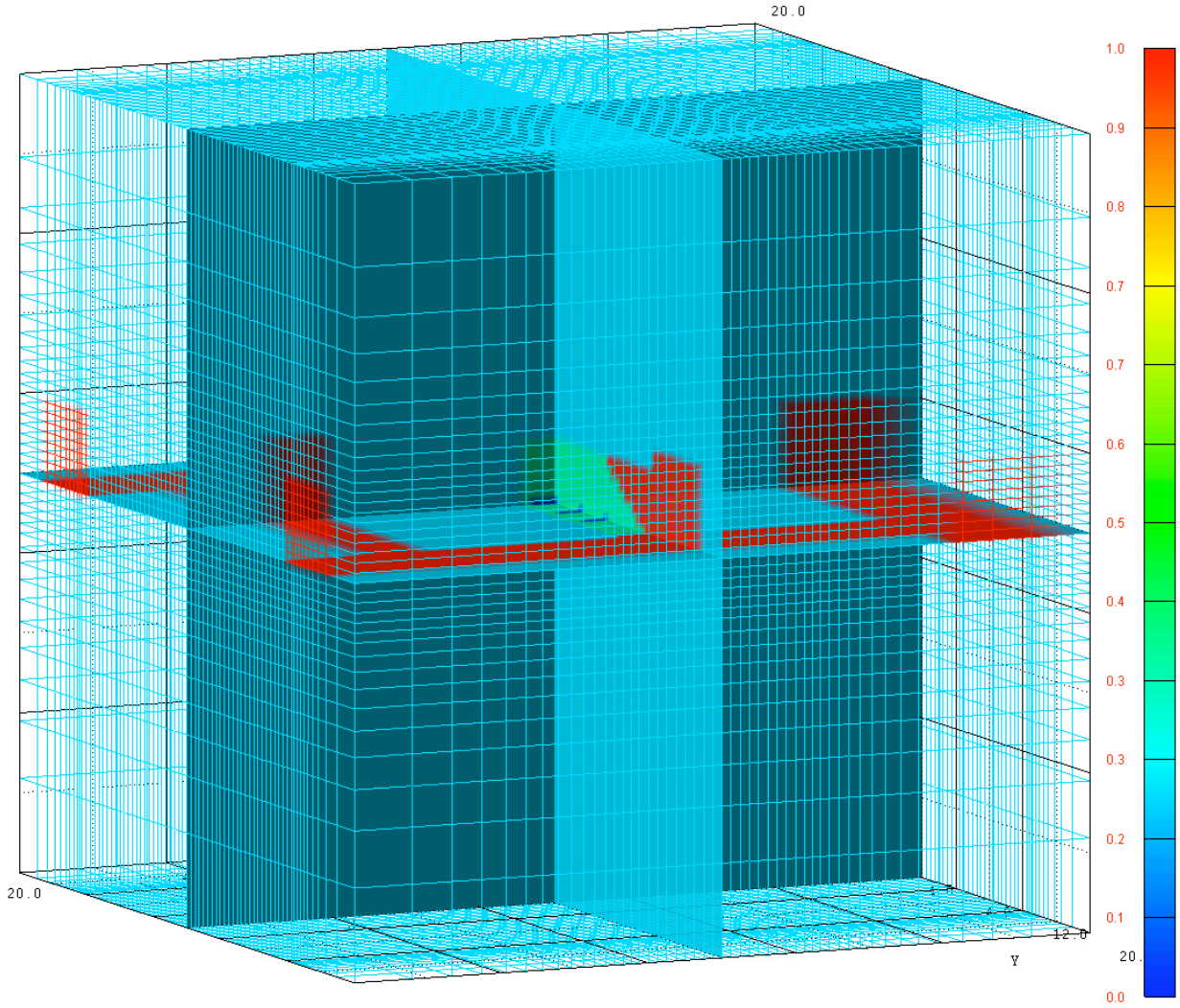

Figure VI.1 Porosity mapped onto slice planes of the numerical mesh for the proof-of-concept drift scale heater simulations. Access drifts and the outer edge of the experimental drift can be seen as red (porosity = 1.0), while the crushed salt backfill can be seen as the sloping green region with porosity of 0.35.

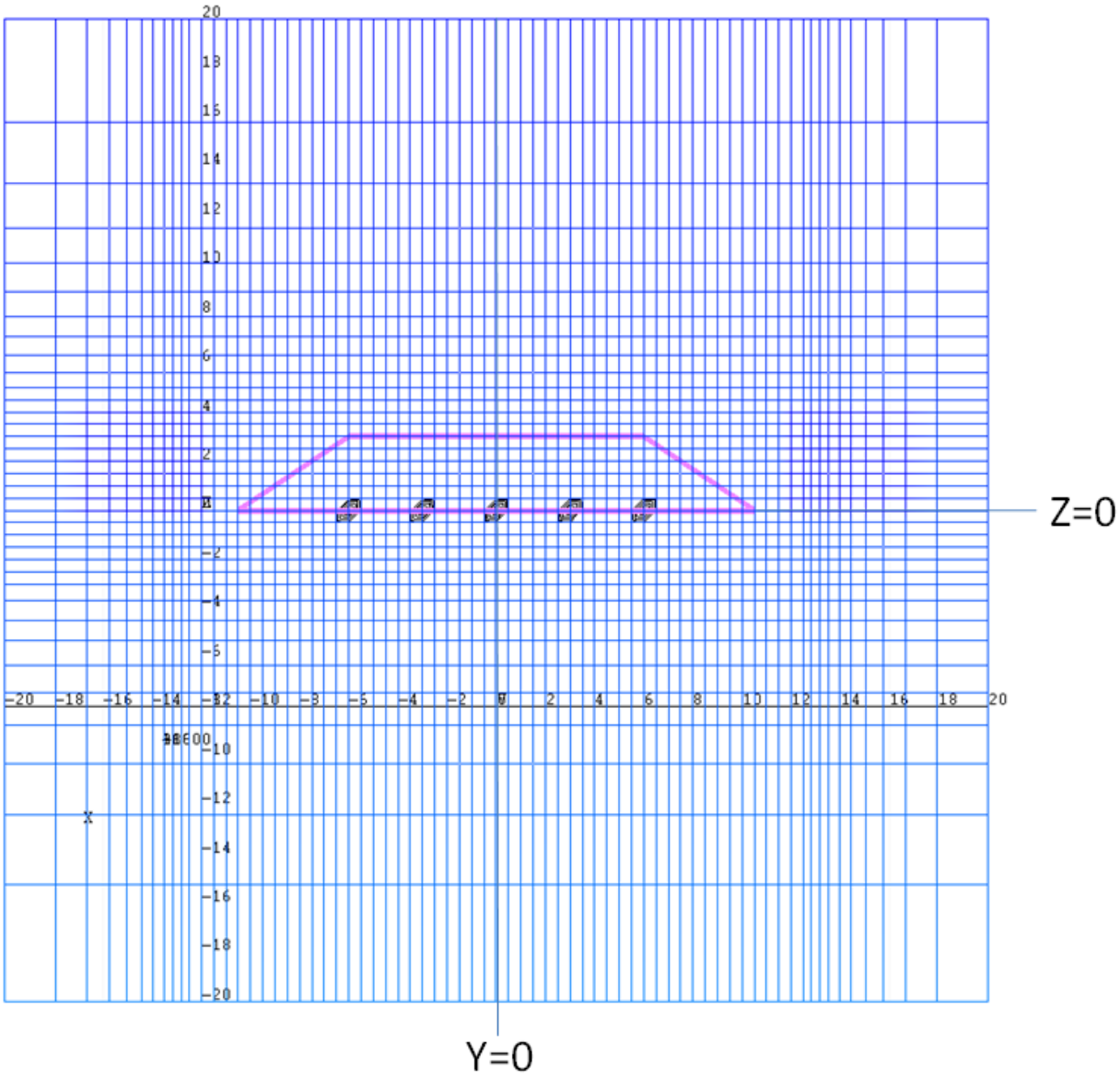

Figure VI.2 Numerical mesh on the XZ plane. The five heaters can be seen in the middle of the mesh, lying under a pile of run-of-mine salt used as backfill (pink trapezoid).

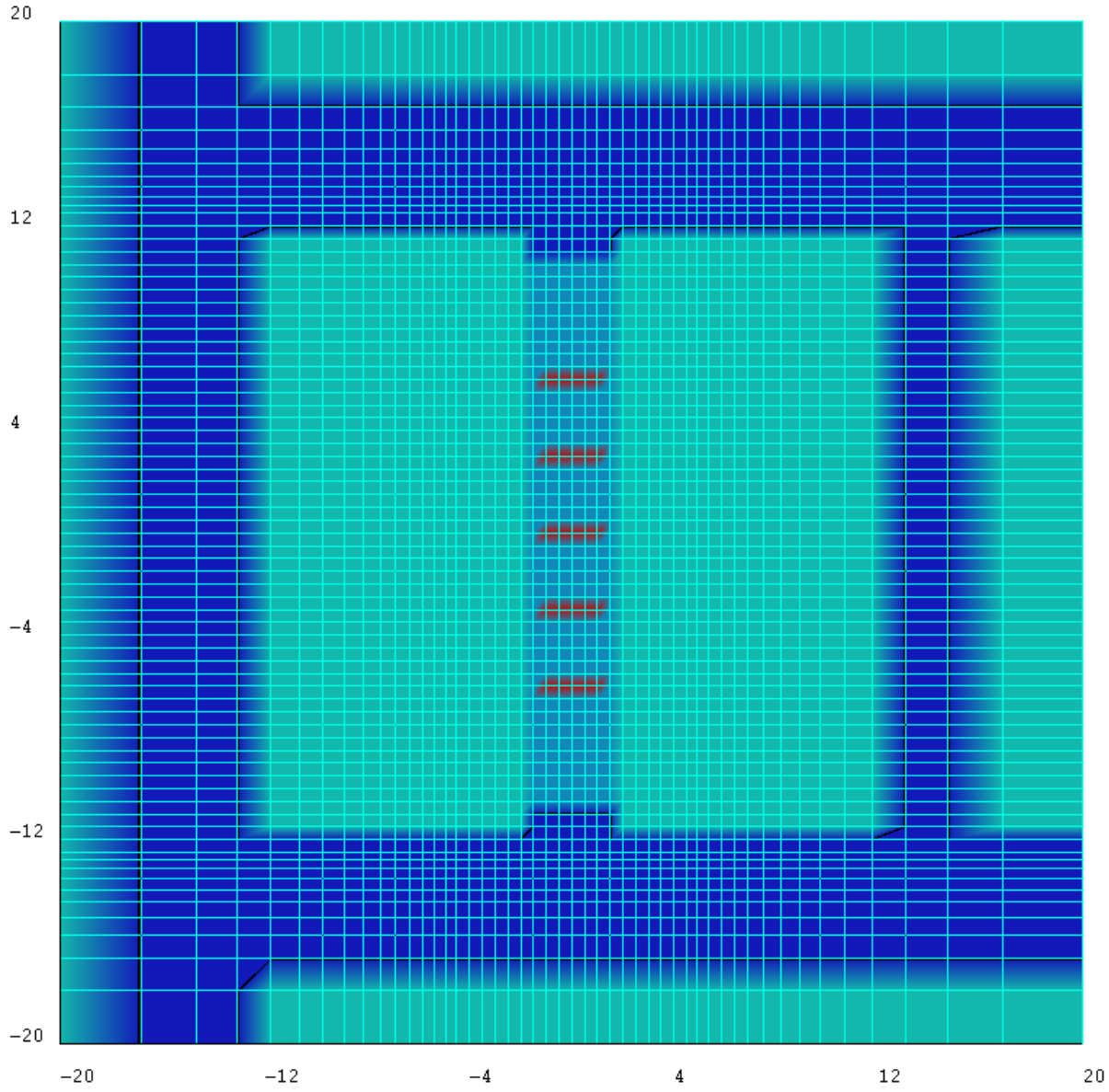

Figure VI.3 Numerical mesh on the XY plane at Z=0. The five heaters can be seen in the middle of the mesh. The access drifts are dark blue around the perimeter of the domain, while the experimental drift lies directly in the center and is lighter blue where the run-of-mine salt backfill is located.

b. Drift scale heater test simulation results

Data on existing thermally active waste containers from around the DOE complex suggest heat loads that could vary from less than 100 W per package to some with over 2000 W per package (Carter et al. 2012). Thus simulations are presented for a range of heating scenarios (Figures VI.4 – VI.6).

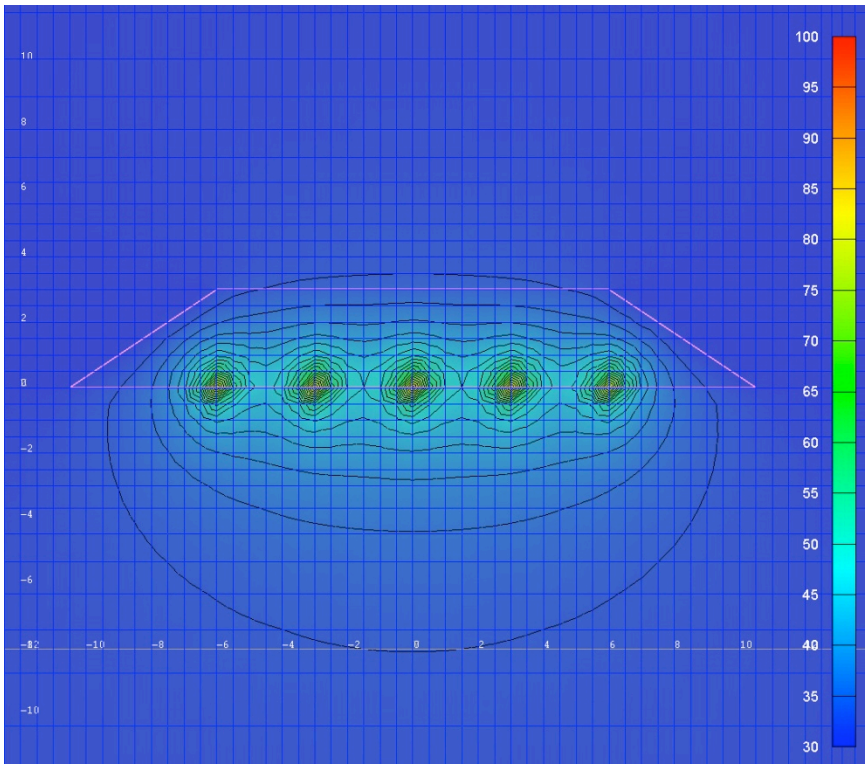

Figure VI.4 Temperature profile near steady state (1 yr) for five 500W heaters.

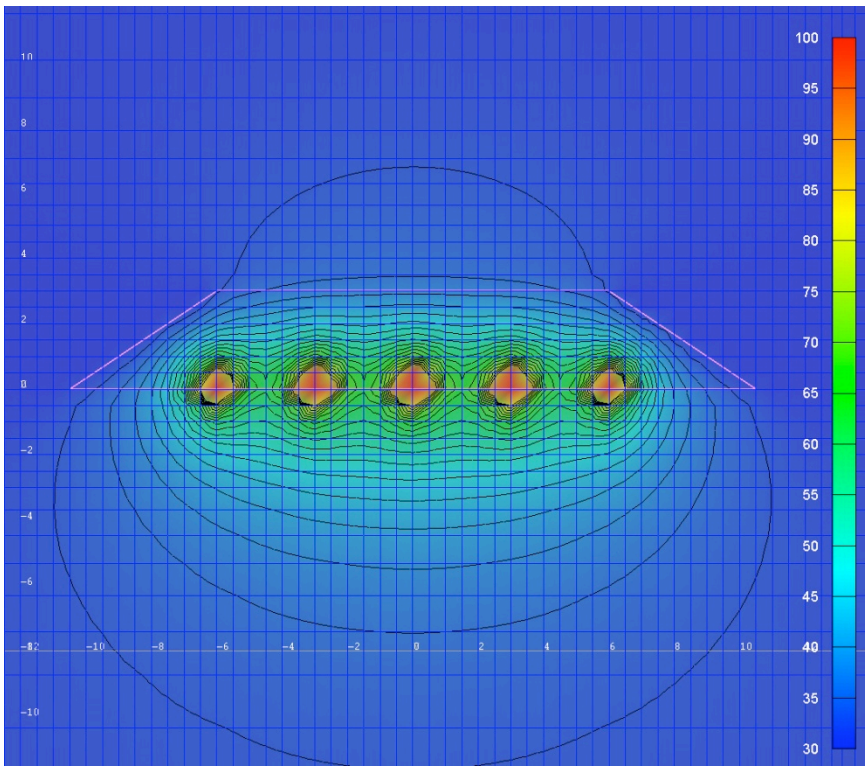

Figure VI.5 Temperature profile near steady state (1 yr) for five 1000W heaters.

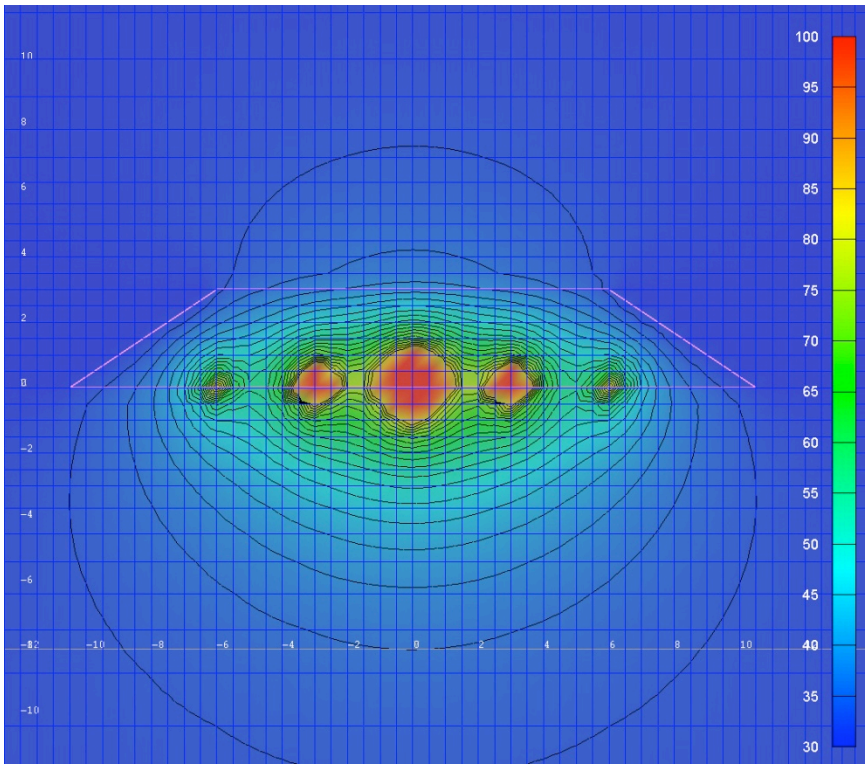

Figure VI.6 Temperature profile near steady state (1 yr) for five heaters with variable loads ranging from 2000W in the center, 1000W adjacent to the center, and 500W on the outer edges.

Temperature gradients of the sort presented in these figures serve as a prelude to understanding the potential water migration issues in either a field experiment with electrical resistance heaters or an actual repository scenario. As air moves through the porous run-of-mine salt that covers the heaters, it will become saturated with water vapor at the local thermodynamic conditions (temperature, fluid ionic strength), as long as there is liquid water present. As the air moves from a warmer to a cooler location, there will be a driving force for water condensation. Water source terms include the initial water present in the run-of-mine salt, as well as the seepage of water toward the drift from the surrounding intact salt. Thus, the bulk migration of water as liquid and vapor in the vicinity of the heaters (or waste packages) is subject to multiple processes, including pressure and temperature-driven flow into the drift, vaporization, and advective transport in the air phase, and possibly condensation in cooler regions due to supersaturated conditions. One of the main purposes of a field test is to demonstrate an understanding of the interplay of these processes that is sufficient to develop a quantitative model of the overall water balance during the first few years of heating.

VII. Conclusions

Benchmarking studies of FEHM against analytical solutions for brine flow to a borehole in salt show mixed results that are being further examined to determine to evaluate the source of discrepancies identified for some of the comparisons. For the isothermal case, the match is nearly perfect. For the heated case, FEHM contains permeability feedback

that result in radically different results from the more simple analytical solutions. However, isothermal calculations of flow into large diameter boreholes done using FEHM and the analytical solutions both yield much higher estimates of salt permeability ($1.0x10^{-18}$ m^2) than were reported by Nowak from their thermal analytical model ($5.0x10^{-21}$ m^2). These higher permeabilities are more in line with values that were calculated by LANL using the thermal analytical model. The lower permeability results fit well for small diameter boreholes, and this result suggests that the larger diameter boreholes may have higher near-field permeability than the small diameter boreholes. Such a difference could be the result of a larger damaged zone due to higher stresses and vibrations encountered when drilling large diameter boreholes.

Thermal modeling of drift scale heater experiments shows that temperature perturbations will likely lead to local liquid/vapor convection over time-scales of decades. Such convection could lead to higher liquid saturations accumulating in the relatively cool regions in between the emplaced heaters. Future simulations will explicitly model the water fate and transport under these conditions.

VIII. References

Clayton, D.J. and C.W. Gable(2009). 3-D Thermal Analyses of High-Level Waste Emplaced in a Generic Salt Repository, Advanced Fuel Cycle Initiative, AFCI-WAST-PMO-MI-DV-2009-000002, SAND2009-0633P. LA-UR-09-0089.

J. T. Carter, A. J. Luptak, J. Gastelum, C. Stockman, and A. Miller, 2012. Fuel Cycle Potential Waste Inventory for Disposition, Fuel Cycle Research & Development Report FCR&D-USED-2010-000031 Rev 5.

J. Crank, The Mathematics of Diffusion. Clarendon Press, Oxford, 1979, p. 87. .

D. E. Deal and J. B. Case, IT Corporation, Brine Sampling and Evaluation Program. Phase I Report. DOE-WIPP-87-008, prepared by the Engineering and Technology Department of the Management and Operating Contractor, Waste Isolation Pilot Plant Project for the U. S. Department of Energy, June 1987. .

E. J. Nowak, D. F. McTigue and R. Beraun, Sandia Report SAND88-0112, Brine Inflow to WIPP Disposal Rooms: Data, Modeling, and Assessment, prepared by Sandia National Laboratories, September 1988. .

FEHM. (2012). FEHM reference list, online at http://fehm.lanl.gov/pdfs/FEHM_references_list.pdf, accessed Aug. 31, 2012. .

A. F. Gangi (1978), Variation of whole and fractured porous rock permeability with confining pressure, Rock Mech. Sci. and Geomech. Abstr. 15: 249-257.

GRIDDER (2012). Gridder Users Manual, (Loraine Lundquist), on-line at https://meshing.lanl.gov/gridder/users_manual.html accessed Aug. 31, 2012. .

D. F. McTigue (1985), A linear theory for porous thermoelastic materials, SAND85-1149, Sandia National Laboratories, September 1985.

Munson, DE, RL Jones, JR Ball, RM Clancy, DL Hoag and SV Petney. 1990. *Overtest for Simulate Defense High-Level Waste (Room B): In Situ Data Report (May 1984-February 1988) Waste Isolation Pilot Plant (WIPP) Thermal/Structural Interactions Program*, Sandia National Laboratories, SAND89-2671. .

Zyvoloski, G.A.(2007). *FEHM: A control volume finite element code for simulating subsurface multi-phase multi-fluid heat and mass transfer*, Report LA-UR-07-3359, Los Alamos National Laboratory.